AD-A071 658 ATOMIC ENERGY RESEARCH ESTABLISHMENT HARWELL (ENGLAND) F/G 11/6
STRUCTURAL EXAMINATION OF COLD ROLLED M316 AUSTENITIC STAINLESS--ETC(U)
FEB 79 M W BOWKETT

UNCLASSIFIED AERE-R-9361 NL

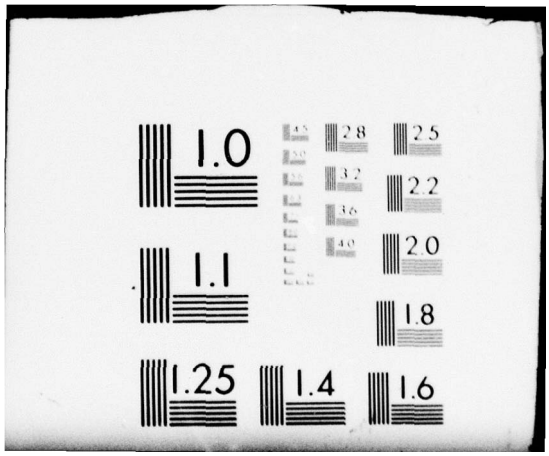
1.0
1.1
1.25
1.4
1.6
1.8
2.0
2.2
2.5
2.8
3.2
3.6
4.0

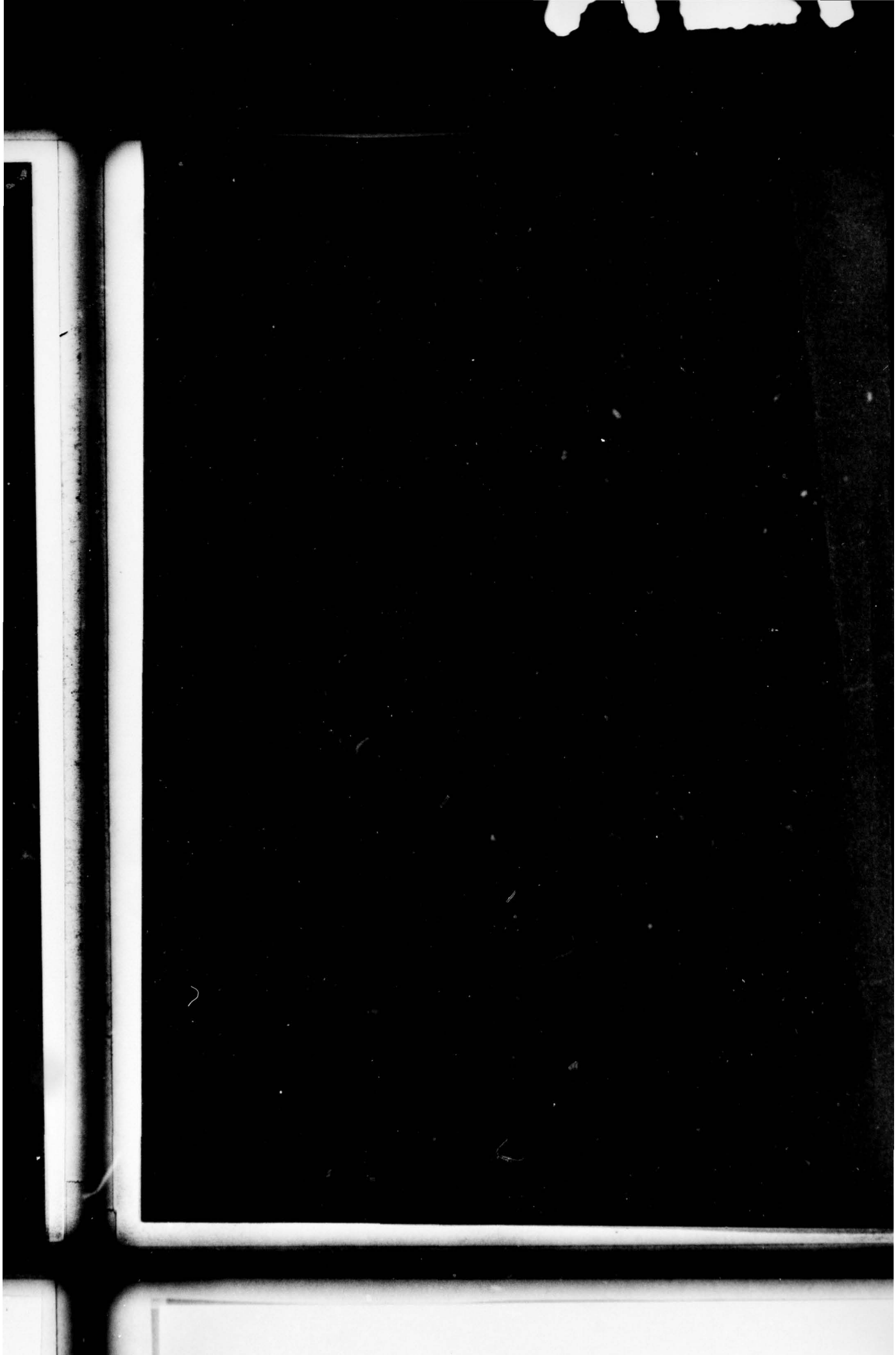

(14) AERE-R-9361
HL79/518

(6) Structural Examination of Cold Rolled M316 Austenitic Stainless Steel

by

(10) M. W. Bowkett

ABSTRACT

The structures of solution treated and cold worked M316 austenitic steel have been investigated using magnetic measurements, optical and transmission electron microscopy and electron, X-ray and neutron diffraction. The results show that the steel is resistant to both ε- and α'-martensite formation during ambient temperature rolling to deformations of up to 50% and this is attributed to its relatively high stacking fault energy. The banded structures observed in the cold worked steel have been positively identified by electron diffraction and high resolution dark field techniques as deformation twins.

* eta

** alpha'

Metallurgy Division,
AERE Harwell.

(11) Feb[illegible]1979

HL79/518 (C.14)

(12) 23p.

*046 500

CONTENTS

ILLUSTRATIONS

1. X-ray diffraction patterns (MoK_{α}) of solution treated and cold worked M316 steel.

2. Neutron diffraction spectra of solution treated and cold worked M316 steel.

3. 5% cold worked M316 steel. Transmission electron micrographs.

   (a). Bright field (BF) micrograph.
   (b). Selected area electron diffraction pattern (SADP).
   (c), (d), (e) and (f). High resolution dark field micrographs (HRDF).

4. 20% cold worked M316 steel. Transmission electron micrographs.

   (a). BF micrograph
   (b). SADP
   (c). SADP
   (d), (e), (f), (g), (h) and (i). HRDF micrographs.

5. 50% cold worked M316 steel. Transmission electron micrographs.

   (a). BF micrograph
   (b). SADP
   (c), (d), (e), (f), (g) and (h). HRDF micrographs.

6. Solution treated M316 steel. Transmission electron micrograph.

7. Optical micrographs of the solution treated and cold worked M316 steel.

8. Superimposed computer-simulated electron diffraction patterns for the fcc γ/twinning and fcc γ/hcp ε relationships in the $[\bar{1}01]_{\gamma}$ ((a) and (b)) and $[\bar{1}14]_{\gamma}$ ((c) and (d)) matrix orientations.

1. INTRODUCTION

M316 austenitic steel (specified composition (wt.%) - 0.03-0.06 C, 0.60 max. Si, 1.5-2.0 Mn, 16.5-17.5 Cr, 13-14 Ni, 2.00-2.75 Mo, balance essentially Fe) is the reference fuel element cladding material for the U.K. Prototype Fast Reactor (PFR)[1][2]. M316 and some of the other fast reactor core component materials, such as Type 321 (En58B) austenitic steel[2], are used in the solution treated and 20% cold worked condition. The possibility that transformation of the austenite to martensitic phases may occur during the cold deformation[3][4] and influence the irradiation induced void swelling and dimensional stability of the alloys has prompted extensive investigations of the constitution and the deformation induced structures in these materials.

The effects of deformation on the transformation of austenite to martensite in a number of commercial austenitic steels, including some of the AISI 300 series, have been studied by Llewellyn and Murray[5]. They established that the extent of the transformation of the austenite to the ferromagnetic, body-centred-cubic (b.c.c.) α'-martensite during ambient temperature deformation decreased with increasing amounts of Ni, Mn and Cu, the Ni having the most powerful effect. Thus, the Type 316 (compositional ranges investigated (wt.%) - 0.04-0.06 C, 0.23-0.32 Si, 1.70-1.92 Mn, 17.02-18.40 Cr, 11.2-11.6 Ni, 2.65-2.86 Mo, 0.019-0.036 N) and other austenitic steels containing 17-18 wt.% Cr and $\geq$ 11.5 wt.% Ni were completely resistant to α'-martensite formation during rolling by up to 70% reductions at ambient temperature. Although, the $\gamma \rightarrow \alpha'$-martensite transformation could not be induced simply by quenching to -196°C, $\sim$ 60% α' was, however, formed in the Type 316 steel during tensile straining at this temperature. Llewellyn and Murray concluded from X-ray diffraction analyses that small amounts of the non-magnetic, hexagonal-close-packed (hcp) ε-martensite were formed in the Type 316 steel on deforming in the range 21-51% at room temperature.

Mazza[6] observed bands in a Type 316 steel (analysis (wt.%) - 0.05 C, 0.52 Si, 1.29 Mn, 16.4 Cr, 11.1 Ni, 2.46 Mo) by TEM following $\geq$ 12% tensile deformation at room temperature; these bands were identified by electron diffraction as deformation twins on $\langle 111 \rangle_\gamma$ planes in $\langle 112 \rangle_\gamma$ directions. Furthermore, he found that the region near the fracture of the tensile specimen was strongly magnetic and X-ray diffraction analysis indicated that this was due to α'-martensite formation. Again, the α' could not be induced merely by quenching to -196°C and there was no evidence of

ε formation.

Blenkinsop and Nutting[7] have reported that both deformation twins and ε-martensite were observed by TEM in a Type 316L austenitic steels (analysis (wt.%) - 0.03 C, 0.57 Si, 1.56 Mn, 16.7 Cr, 13.08 Ni, 2.43 Mo) after ≥ 10% deformation at room temperature. Furthermore, Garr et al[8] have claimed that ε-martensite was present in a 25% cold rolled Type 316 steel (analysis (wt.%) - 0.06 C, 17.3 Cr, 13.6 Ni, 2.3 Mo, 0.05 N). Partial reversion of the ε-martensite to austenite was detected after subsequent ageing at 480°C for 24h; this latter observation is somewhat dubious in view of the fact that complete reversion of ε to γ is reported to occur within the range 150°-400°C, even after short annealing times[4]. α'-martensite was not detected by Blenkinsop and Nutting[7] nor Garr et al[8] in their respective steels.

Larbalestier[9] studied the effects of cryogenic cycling on the magnetic properties of a series of austenitic steels, including Type 316LN (analysis (wt.%) - 0.05 C, 0.38 Si, 1.49 Mn, 16.77 Cr, 12.43 Ni, 2.4 Mo, 0.18 N, 0.02 P and 0.03 S). Repeated cycling from room temperature to -196°C failed to induce α'-martensite formation in this steel; it was claimed that the absence of α', as well as ε-martensite transformation was confirmed by optical metallographic observations, but it is doubtful if this conclusion is justified in view of the difficulties in positively identifying these phases by optical microscopy. It was also reported that repeated quenching to -269°C failed to induce the α'-martensite transformation in this steel.

There is thus general agreement that Type 316 austenitic steels are resistant to α'-martensite formation during ambient temperature deformation; Mazza's[6] detection of α' may well be due to the slightly lower nickel content (11.1 wt.%) of his Type 316 steel. It is furthermore established that quenching to liquid nitrogen temperature (or even to -269°C, according to Larbalestier's[9] findings) does not promote transformation of γ to α' but the transformation can be induced by deformation at -196°C. However, it is evident that there is some conflict with respect to the formation of ε-martensite and/or deformation twins in Type 316 steel during ambient temperature deformation.

Structural examinations of M316 austenitic steel in the solution treated and cold rolled conditions have been carried out using a combination of magnetic measurements, optical and transmission electron microscopy and electron, X-ray and neutron diffraction in an attempt to resolve some of these uncertainties.

2. EXPERIMENTAL DETAILS

2.1 Materials and Thermomechanical Treatments

The cast (Ingot No. 8/22230) analysis of the M316 steel in wt.% was as follows:- 0.05 C, 0.35 Si, 1.77 Mn, 17.0 Cr, 13.5 Ni, 2.36 Mo, 0.028 N, 0.01 P, 0.008 S. The steel was originally supplied in the form of 0.125 in. (3.175 mm) thick wrapper plates which were rolled at ambient temperature, with intermediate solution treatment at 1050°C, to a standard thickness of 0.032 in. (0.81 mm); the rolling and annealing schedules were adjusted such that strips with reductions in the range 0 to 50% were produced.

The stability of austenitic steels with respect to α'-martensite formation is indicated by the M_{s_α}, (the temperature at and below which spontaneous transformation of $\gamma \rightarrow \alpha'$ occurs on quenching) and the M_{d_α}, (the temperature above which the transformation cannot be induced by deformation irrespective of the strain) temperatures. These temperatures have been related to composition by a number of empirical formulae, each applicable to specific austenitic steel compositional ranges[3]. Thus, the M_{s_α}, temperatures estimated by substituting the elemental compositions of the M316 steel in the formulae given by Eichelman and Hull[10] and Holmes et al[11] suggest that the $\gamma \rightarrow \alpha'$-martensite transformation will not be induced in this steel even by quenching to liquid helium temperature. However, the equations derived by Angel[12] and Williams et al[13] give M_{d_α}, (30/50) (the temperature at which 50% α' is formed after a true tensile strain of 30%) and M_{d_α}, (45/10) (the temperature at which 10% α' is formed after a true compressive strain of 45%) temperatures of -49° and -131°C respectively for the M316 steel, thereby implying that α'-martensite formation should only be produced during deformation at sub-ambient temperatures.

2.2 Experimental Techniques and Results

The experimental techniques employed have been detailed previously[3]. The magnetic measurements confirmed that no α'-martensite was produced in the samples deformed by up to 50% by rolling at ambient temperature. Furthermore, the presence of peaks due to the α'- and ε-martensite phases could not be detected in the X-ray and neutron diffraction spectra of the cold worked samples (Figs. 1 and 2 respectively).

However, TEM showed banded structures in the cold rolled specimens (Figs. 3(a), 4(a) and 5(a)) which were absent in the solution treated sample (Fig. 6). The morphologies of these banded structures are similar to those of the ε-martensite and/or deformation twins observed previously in the cold rolled Type 321 (En58B) austenitic steel[3]. The deformation bands were also visible by optical microscopy, particularly after 50% deformation (Fig. 7).

From the electron diffraction work of Kestenbach[14] and using a computer programme[15] designed to plot superimposed electron diffraction patterns for known orientation relationships[16], it was possible to isolate specific fcc matrix orientations in which the ε-martensite bands and deformation twins could be positively distinguished. Two such orientations are (i) a $\langle 110 \rangle_\gamma$ in which the extra twin reflections constitute a $\langle 110 \rangle_\gamma$ pattern whereas the extra ε reflections constitute a $[1\bar{2}10]_\varepsilon$ pattern and (ii) a $\langle 114 \rangle_\gamma$ in which the extra twin reflections constitute a $\langle 110 \rangle_\gamma$ pattern whereas the ε reflections constitute a $[\bar{2}20\bar{3}]_\varepsilon$ pattern which completely overlaps with the $\langle 114 \rangle_\gamma$ matrix pattern. Computer-simulated electron diffraction (CSD) patterns for specific variants of these two matrix orientations ($[\bar{1}01]_\gamma$ and $[114]_\gamma$) with their respective twin and/or ε patterns are shown in Fig. 8; they were constructed using the following orientation relationships:-

fcc γ/twinning

$$(111)_\gamma \;||\; (111)_T$$
$$[\bar{1}01]_\gamma \;||\; [10\bar{1}]_T$$
$$[01\bar{1}]_\gamma \;||\; [0\bar{1}1]_T$$

fcc γ/hcp ε

$$(111)_\gamma \;||\; (0001)_\varepsilon \;\text{OR}\; (00.1)_\varepsilon$$
$$[\bar{1}01]_\gamma \;||\; [1\bar{2}10]_\varepsilon \;\text{OR}\; [1\bar{2}.0]_\varepsilon$$
$$[01\bar{1}]_\gamma \;||\; [\bar{2}110]_\varepsilon \;\text{OR}\; [\bar{2}1.0]_\varepsilon$$

The selected area electron diffraction (SAD) and high resolution dark field (HRDF) evidence illustrated in Figs. 3, 4 and 5 confirms that the banded structures are deformation twins and not ε-martensite bands; the twins form on $\{111\}_\gamma$ planes in $\langle 112\rangle_\gamma$ directions consistent with Mazza's[6] findings and the twinning planes and directions normally exhibited by fcc metals and alloys[17]. After 5% deformation, the twins in the bright field (BF) micrograph (Fig. 3(a)) give rise to a $\langle 110\rangle_T$ SAD pattern in a $\langle 110\rangle_\gamma$ matrix zone (Fig. 3(b)) which agrees with the CSD patterns in Fig. 8(a); the matrix and twin reflections yield the HRDF micrographs shown in Figs. 3(c), (d) and 3(e), (f) respectively. After 20% deformation, the twins in the BF micrograph (Fig. 4(a)) produce an apparent single SAD pattern (Fig. 4(c)) which, in fact, consists of two patterns, the $\langle 114\rangle_\gamma$ and the $\langle 110\rangle_T$ which comply with the CSD patterns in Fig. 8(c); the twin reflections give the HRDF micrographs in Figs. 4(d), (e) and (f) whereas the overlapping matrix and twin reflections result in the HRDF micrographs shown in Figs. 4(g), (h) and (i). Fig. 4(b) illustrates a $\langle 114\rangle_\gamma$ matrix pattern obtained from the twin-free area (b) in Fig. 4(a). Finally, after 50% deformation, the twins in Fig. 5(a) again produce a $\langle 110\rangle_T$ pattern in a $\langle 114\rangle_\gamma$ matrix zone (Fig. 5(b)) and the twin reflections yield the HRDF micrographs in Figs. 5(c), (d) and (e) whereas the overlapping matrix and twin reflections give the HRDF micrographs in Figs. 5(f), (g) and (h).

3. DISCUSSION

3.1 α'- and ε- Martensite Formation

The observed resistance of the M316 austenitic steel to α'-martensite transformation during ambient temperature deformation is consistent with the results of most of the previous work on similar 316 type steel compositions[5][7][8] and, in accord with Llewellyn and Murray's[5] findings, may be attributed to its relatively high nickel content of 13.5 wt.%. Furthermore, the absence of ε-martensite formation in the M316 steel agrees with Mazza's[6] observations but conflicts with Llewellyn and Murray's X-ray diffraction data[5], Blenkinsop and Nutting's TEM results[7] and the reported presence of this phase by Garr et al[8] in Type 316 steels. However, in view of

the difficulties inherent in the detection of ε-martensite by X-ray diffraction[3] and in conclusively distinguishing between ε-martensite and deformation twins by electron diffraction, the previous reports of the formation of ε-martensite in 316 type steels deformed at ambient temperatures must be treated with some scepticism.

3.2 Deformation Twinning and ε-Martensite

The deformation stacking faults on close packed {111} planes in f.c.c. crystals are of two fundamental types, intrinsic and extrinsic; the former comprises one violation and the latter two violations in the atom stacking sequence. If the normal fcc stacking sequence is represented as ABCABCABC and the respective symbols Δ and ∇ are used to denote normal stacking (AB,BC and CA) and reverse stacking or a violation (AC,CB and BA)[17], then these two faults can be illustrated thus:-

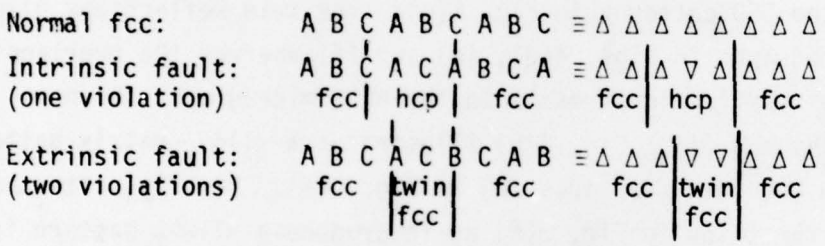

It is noted that intrinsic faults on alternate close packed $\{111\}_{fcc}$ planes produce the hcp structure (CACA) whereas twinning is produced by intrinsic faults on every close packed plane (or extrinsic faults on alternate close packed planes since these can be considered essentially as two intrinsic faults on adjacent planes[18,19]). Therefore, a thicker hcp region and a thicker twin may be represented thus:

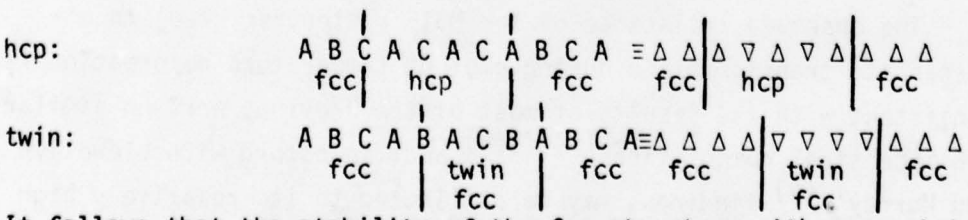

It follows that the stability of the fcc structure with respect to the formation of the hcp ε-martensite should be related to the stacking fault energy (γ_{SFE}) of the alloy.

The majority of γ_{SFE} determinations have been made either by the measurement of the radii of extended dislocation nodes using strong beam, bright field TEM[20] or, more recently, by the application of the weak beam, dark field imaging techniques first employed by Cockayne et al[21][22][23]. The γ_{SFE} of austenitic steels and alloys have been measured using the former technique notably by Dulieu and Nutting[24] and others whilst the latter method has been used by Rhodes and Thompson[25] and Bampton, Jones and Loretto[26]. The techniques and data have been reviewed on several occasions[25][27][28][29] and Schramm and Reed[29] and Rhodes and Thompson[25] have attempted to correlate the γ_{SFE} values with the austenitic steel and alloy compositions. It is generally agreed that γ_{SFE} decreases with increasing Cr (if $\lesssim$ 18 wt.%), N, Co and Si and increases with increasing Cr (if $\gtrsim$ 18 wt.%), Ni, C, Mo, Nb and Cu; however, there is some dispute as to the effect of Mn.

Using linear regression analysis, Schramm and Reed[29] derived four equations relating the γ_{SFE} values, obtained mainly by the strong beam, bright field dislocation node technique, to composition and these have been combined to produce the following relationship:

$$\gamma_{SFE}\ (mJm^{-2}) = 25.7 + (2Ni) - (0.9Cr) + (410C) - (77N) - (13Si) - (1.2Mn) \ldots\ldots (1)$$

where Ni, Cr, etc. are in wt.%.

This work was subsequently criticised by Rhodes and Thompson[24] on the grounds that the strong beam, bright field dislocation node technique can only be used confidently for $\gamma_{SFE} \leqslant 30\ mJm^{-2}$ and that the linear relationship is not obeyed for $\gamma_{SFE} \geqslant 50\ mJm^{-2}$. These authors proposed the following relationships between γ_{SFE} and composition; equations (2) and (3) relate to pure Fe-Ni-Cr ternary alloys containing $\leqslant$ 18% Cr and > 18% Cr respectively and equation (4) refers to commercial austenitic alloys containing $\geqslant$ 18% Cr and significant Mn and Si contents:-

$$\gamma_{SFE} = 17.0 + (2.29Ni) - (0.9Cr) \ldots\ldots (2)$$

$$\gamma_{SFE} = -26.6 + (0.73Ni) + (2.26Cr) \ldots\ldots (3)$$

$$\gamma_{SFE} = 1.2 + (1.4Ni) + (0.6Cr) + (17.7Mn) - (44.7Si) \ldots\ldots (4)$$

where Ni, Cr, etc. are again in wt.%.
Equations (1) and (4) are in fairly good agreement for γ_{SFE} $\lesssim$ 50 mJm^{-2} but equation (1) tends to overestimate the γ_{SFE} at higher values.

The majority of the observations on martensitic transformations in a wide range of pure Fe-Ni-Cr alloys and commercial austenitic steels (Fe : 10 - 25% Cr : 5 - 25% Ni + C, N, Mn, Mo, Si) have been made following quenching to or deforming at -196°C. An attempt[4] at correlating the room temperature γ_{SFE} values derived from equations (1) and (4) with the -196°C phase data has shown that the reported presence of ε-martensite occurs at -196°C only if the γ_{SFE} is below a value of 43 ± 5 mJm^{-2} at room temperature. If it is assumed that the linear temperature dependence of γ_{SFE} (0.05 - 0.08 $mJm^{-2}\ {}^{o}K^{-1}$) obtained from Lecroisey's work[30][31][32] in the range -196°C to room temperature for austenitic alloys containing 18% Cr : 12% Ni, 16% Cr : 13% Ni and 18% Cr : 14% Ni, is applicable to the wider range of compositions considered above, then this γ_{SFE} reduces to 25 - 32 mJm^{-2} at -196°C. Furthermore, the analysis of the more limited data on martensitic transformations in austenitic steels following quenching to or deformation at ambient temperature suggests a room temperature γ_{SFE} of 35 ± 5 mJm^{-2} below which ε-martensite is reported to form[4]. It therefore appears, providing the formation of ε-martensite is solely dependent on γ_{SFE} and bearing in mind the errors involved in estimating this parameter, that at a given temperature, there is a critical γ_{SFE} below which transformation of γ to ε-martensite occurs.

Since the room temperature γ_{SFE} for the M316 steels derived from equations (1) and (4) are 52 ± 5 and 46 ± 5 mJm^{-2} respectively, it follows that ε-martensite should not form in this steel during quenching to or deformation at ambient temperature; this conclusion is in agreement with the present experimental observations. Furthermore, if the transformation sequence is $\gamma \rightarrow SF \rightarrow \varepsilon \rightarrow \alpha'$[4], the the formation of α'-martensite may also be dependent on γ_{SFE}, since it relies on the initial formation of stacking faults and ε-martensite. This, of course,

is not true of situations where the α'-martensite forms directly from the parent austenite[4].

Although there is relatively little difference between stacking fault and twin formation in terms of violations in the normal stacking sequence of the atoms in the {111} planes of the fcc lattice, the observation of extensive twinning in the M316 steel deformed at ambient temperature implies that there are fundamental differences in the respective dislocation mechanisms and that twinning can occur even at high γ_{SFE}. The dislocation reactions leading to twinning in fcc structures have not been unambigucusly established but the many models proposed have been reviewed by Venables[19] and Westlake[33]. Additional work is obviously required on this aspect but this is outside the scope of the present investigation.

4. CONCLUSIONS

4.1 M316 austenitic steel is resistant to both ε- and α'-martensite transformation during ambient temperature rolling to deformations of up to 50%; this is attributed primarily to the relatively high stacking fault energy of the steel.

4.2 The banded structures observed in the cold worked steel by transmission electron microscopy have been identified as deformation twins using electron diffraction and high resolution dark field techniques.

ACKNOWLEDGEMENTS

The author is indebted to Dr. D. R. Harries for his comments on the manuscript and to Mr. F. Cullen (X-ray Diffraction Section, Materials Development Division) and Dr. C. G. Windsor (Neutron Diffraction, Materials Physics Division) for assistance and the provision of facilities.

REFERENCES

1. D. R. Harries, "The Void Swelling Problem in Sodium Cooled Fast Reactors", Proc. Consultant Symposium on "The Physics of Irradiation Produced Voids", Harwell, September, 1974, Ed., R. S. Nelson, AERE Report - R 7934, January, 1975, p.1.

2. D. R. Harries, "The UKAEA Fast Reactor Project Research and Development Programme on Fuel Element Cladding and Sub-Assembly Wrapper Materials",

Proc. Int. Conf., "Radiation Effects in Breeder Reactor Structural Materials", Scottsdale, Arizona, June 1977, Eds., M. L. Bleiberg and J. W. Bennett, Met. Soc. AIME, 1977, p.27.

3. M. W. Bowkett and D. R. Harries, AERE Report-R 9093, April, 1978.

4. M. W. Bowkett and D. R. Harries, AERE Report to be published.

5. D. T. Llewellyn and J. D. Murray, Iron and Steel Inst., Special Report No. 86, 1964, p.197.

6. J. A. Mazza, J. Iron and Steel Inst., 1966, 204 (CCIV), 783.

7. P. A. Blenkinsop and J. Nutting, J. Iron and Steel Inst., 1967, 205 (CCV), 953.

8. K. G. Garr, C. G. Rhodes and D. Kramer, ASTM Special Technical Publication No. 529, 1973, p.109.

9. D. C. Larbalestier, "Magnetisation Studies of Some Cryogenic Alloys", (Ph.D. Thesis), Imperial College, London, April,1970.

10. G. H. Eichelmann and F. C. Hull, Trans. ASM, 1953, 45, 77.

11. B. Holmes, T. Gladman and F. B. Pickering, B.S.C. Research Report PROD/PM/5762/12/72/A, June 1972.

12. T. Angel, J. Iron and Steel Inst., 1954, 177, 165.

13. I. Williams, R. G. Williams and P. C. Capellaro, Proc. 6th Int. Cryogenic Eng. Conf., Grenoble, May 1976, p. 337.

14. H. J. Kestenbach, Metallography, 1977, 10, 189.

15. S. R. Keown and J. A. Whiteman, private communication.

16. M. W. Bowkett and S. R. Keown, AERE Report to be published.

17. R. E. Smallman, "Modern Physical Metallurgy" 3rd Edition, Butterworths, 1970.

18. A. Howie and U. Valdre, Phil. Mag., 1963, 8, 1981.

19. J. A. Venables, Proc. Int. Conf., "Deformation Twinning", Met. Soc. AIME, 1963, 25, 77.

20. M. J. Whelan, Proc. Roy. Soc., 1959, 249A, 114.

21. D. J. H. Cockayne, J. Microsc., 1973, 98, 116.

22. D. J. H. Cockayne, I. L. F. Ray and M. J. Whelan, Phil. Mag., 1969, 20, 1265.

23. I. L. F. Ray and D. J. H. Cockayne, Proc. Roy. Soc., 1971, 325A, 543.

24. D. Dulieu and J. Nutting, Iron and Steel Inst., Special Report No. 86, 1964, p.140.

25. C. G. Rhodes and A. W. Thompson, Met. Trans., 1977, 8A, 1901.

26. C. C. Bampton, I. P. Jones and M. H. Loretto, Acta. Met., 1978, 26, 39.

27. D. V. Neff, T. E. Mitchell and A. R. Troiano, Trans. ASM., 1969, 62, 858.

28. P. C. J. Gallagher, Met. Trans., 1970, 1, 2429.

29. R. E. Schramm and R. P. Reed, Met. Trans., 1975, 6A, 1345.

30. F. Lecroisey and B. Thomas, Phys. Status Solidi(a), 1970, 2, K217.

31. F. Lecroisey, Doctoral Thesis, University of Nancy, France, 1971.

32. F. Lecroisey and A. Pineau, Met. Trans., 1972, 3, 387.

33. D. G. Westlake, Proc. Int. Conf., "Deformation Twinning, Met. Soc. AIME., 1963, 25, 29.

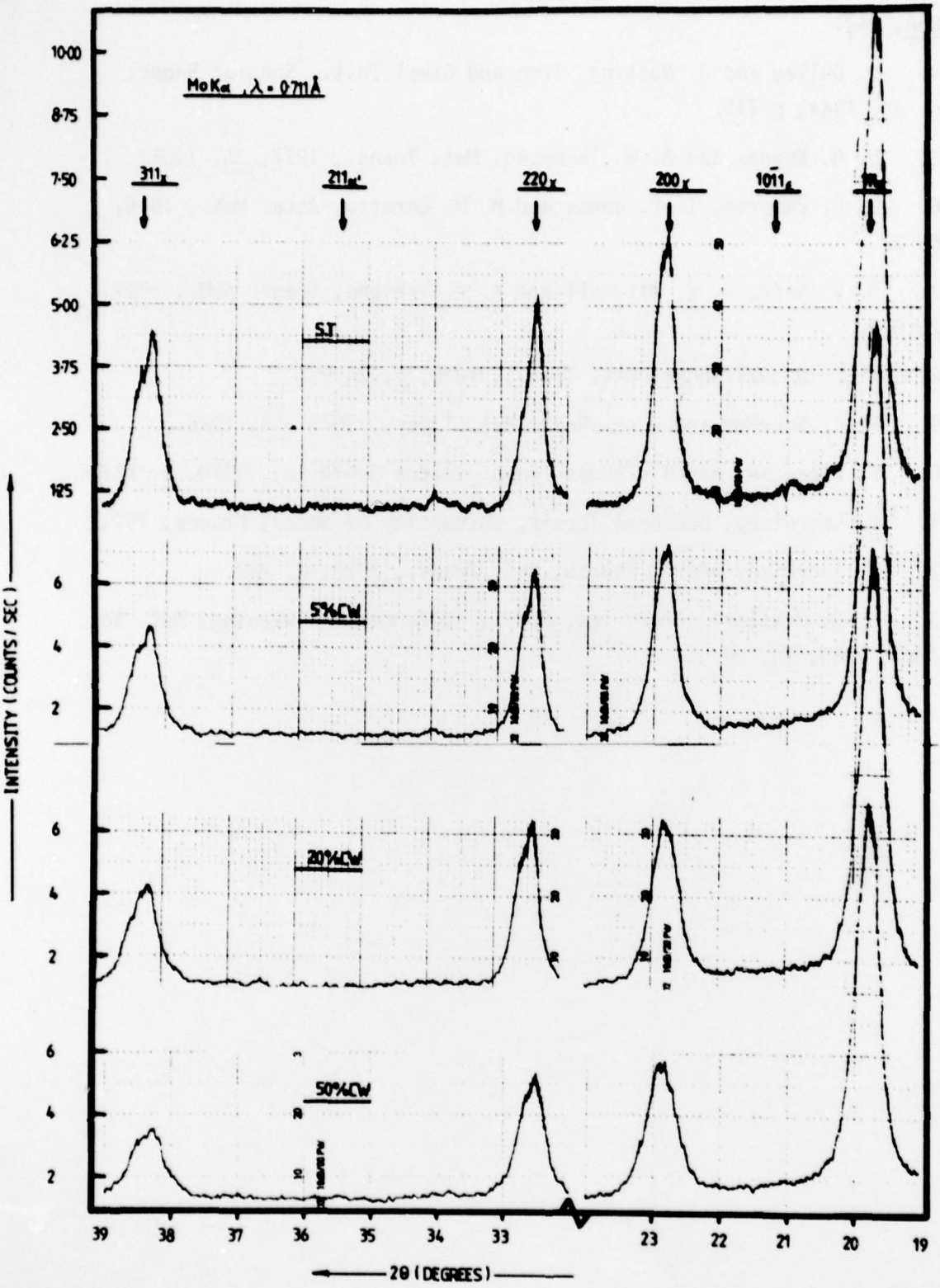

AERE - R 9361 Fig. 1
X-ray diffraction patterns (MoKα) of solution treated and cold worked M316 steel

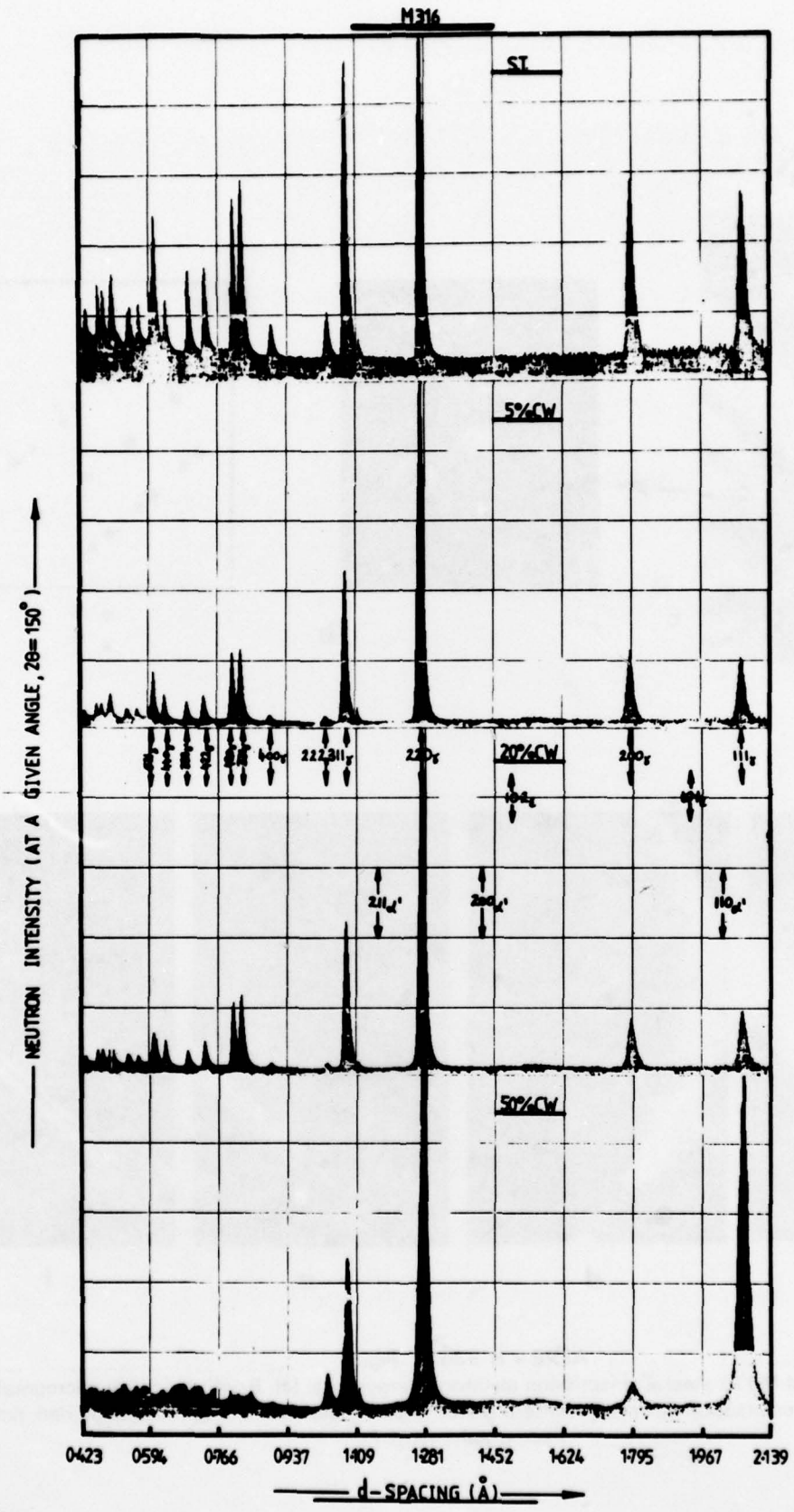

AERE - R 9361 Fig. 2
Neutron diffraction spectra of solution treated and cold worked M316 steel

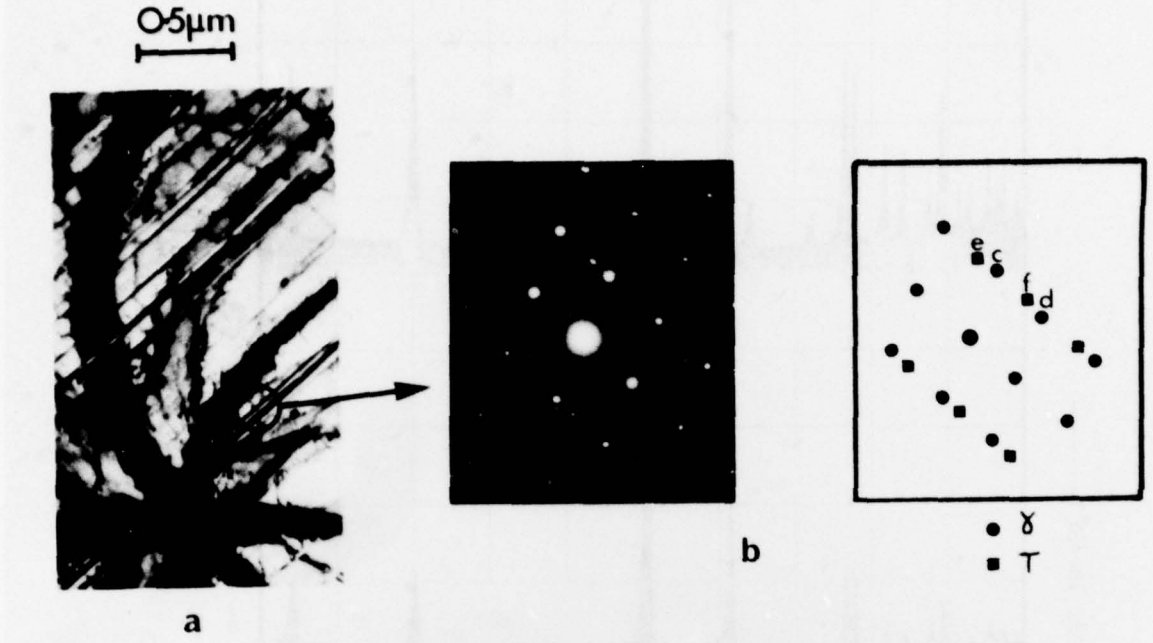

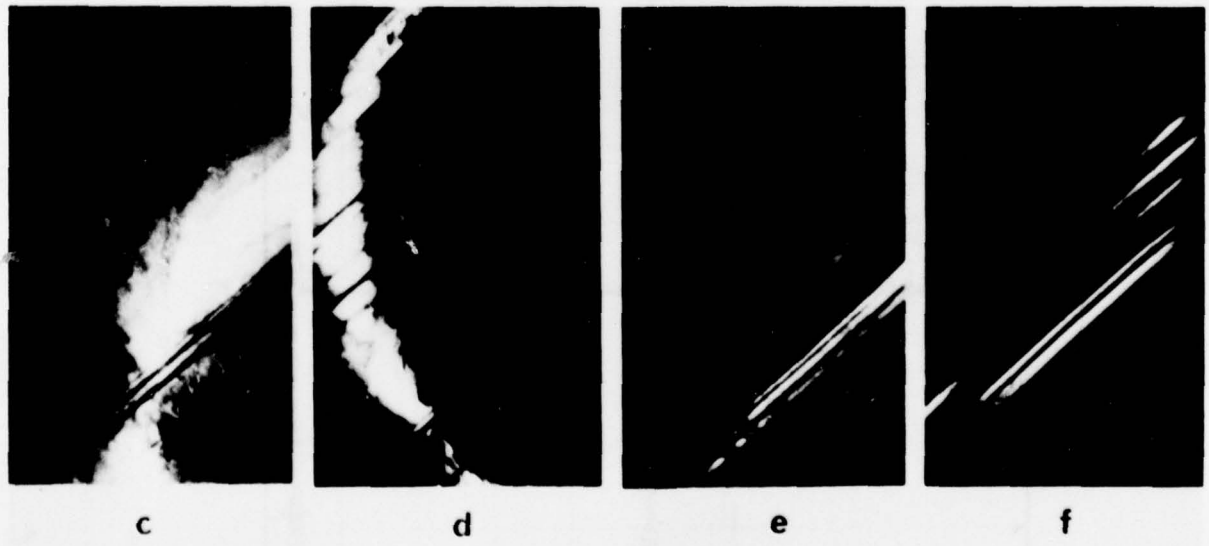

AERE - R 9361 Fig. 3

5% cold worked M316 steel. Transmission electron micrographs. (a) Bright field (BF) micrograph; (b) Selected area electron diffraction pattern (SADP); (c), (d), (e) and (f) High resolution dark field micrographs (HRDF)

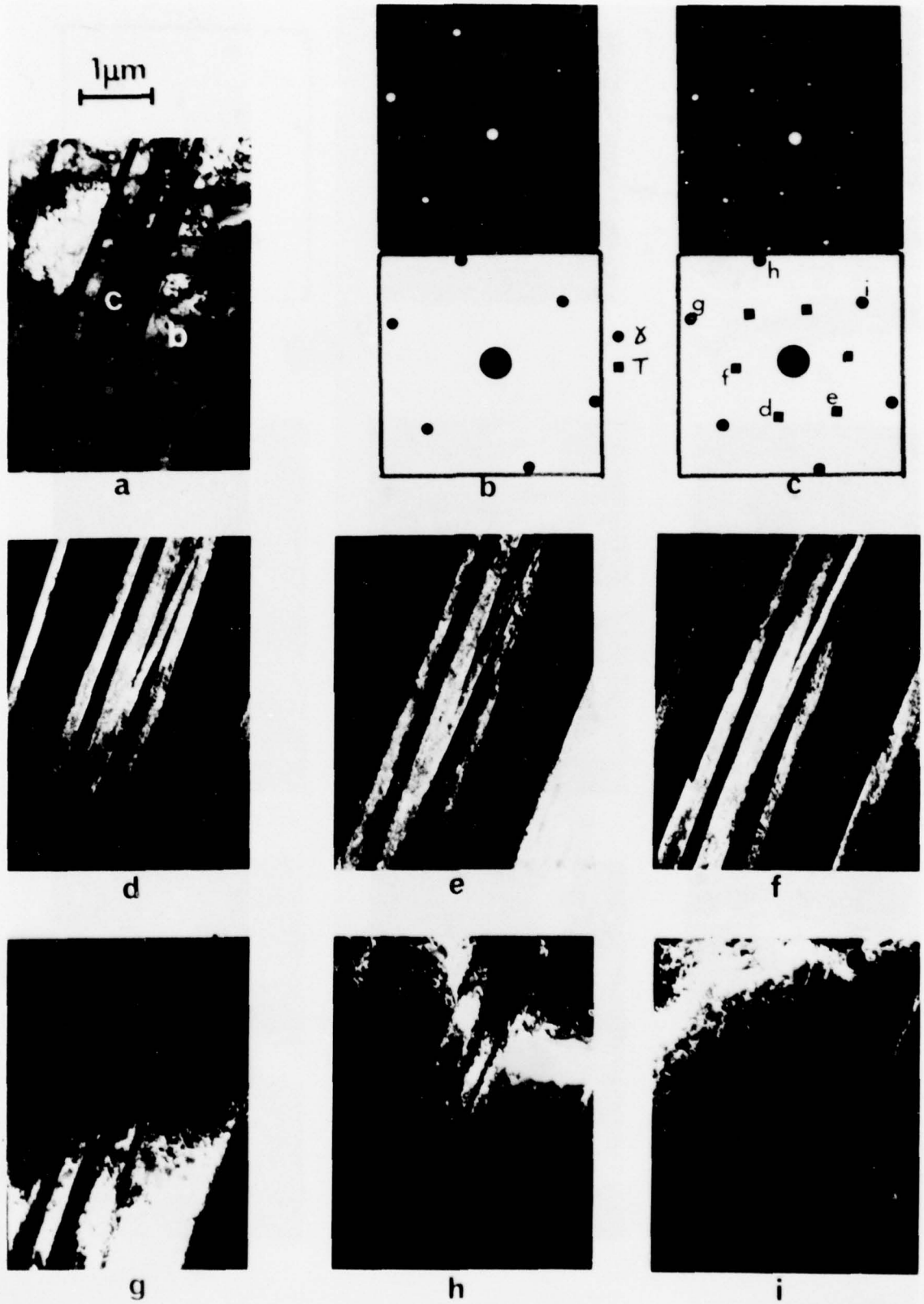

AERE - R 9361 Fig. 4

20% cold worked M316 steel. Transmission electron micrographs. (a) BF micrograph; (b) SADP; (c) SADP; (d), (e) (f), (g), (h) and (i) HRDF micrographs

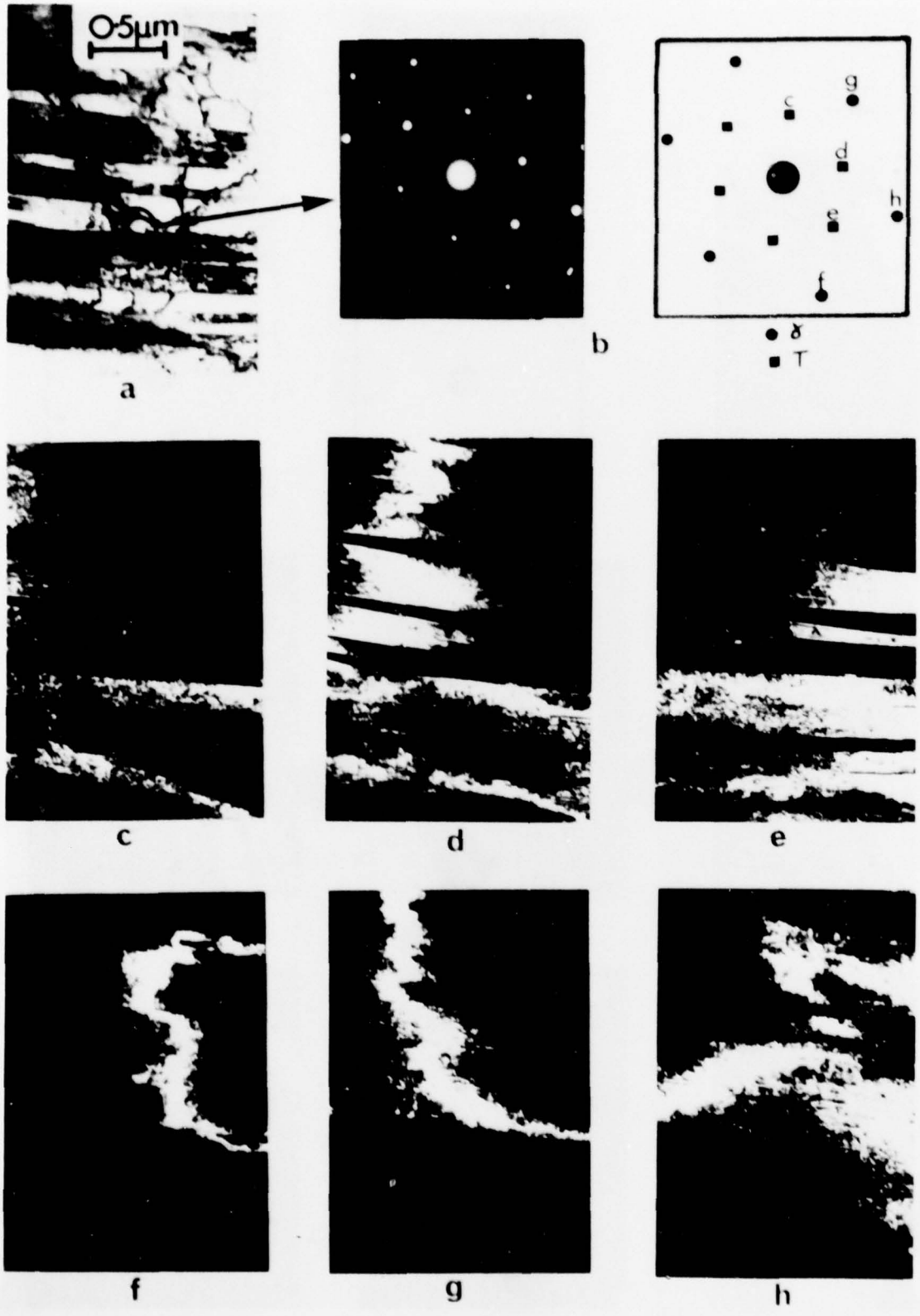

AERE - R 9361 Fig. 5

50% cold worked M316 steel. Transmission electron micrographs. (a) BF micrograph; (b) SADP; (c), (d), (e), (f), (g) and (h) HRDF micrographs

AERE - R 9361 Fig. 6
Solution treated M316 steel. Transmission electron micrograph

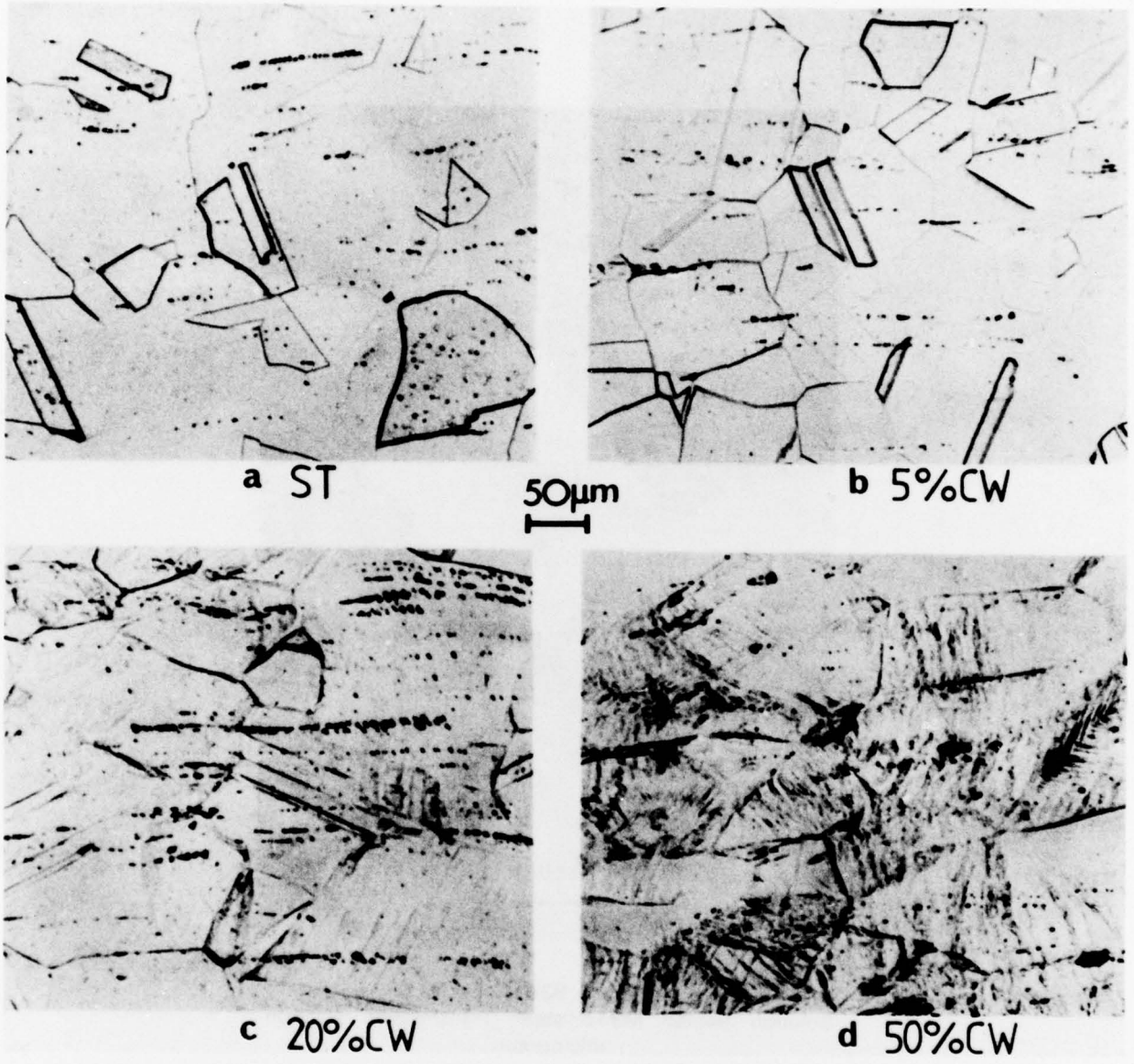

AERE - R 9361 Fig. 7
Optical micrographs of the solution treated and cold worked M316 steel

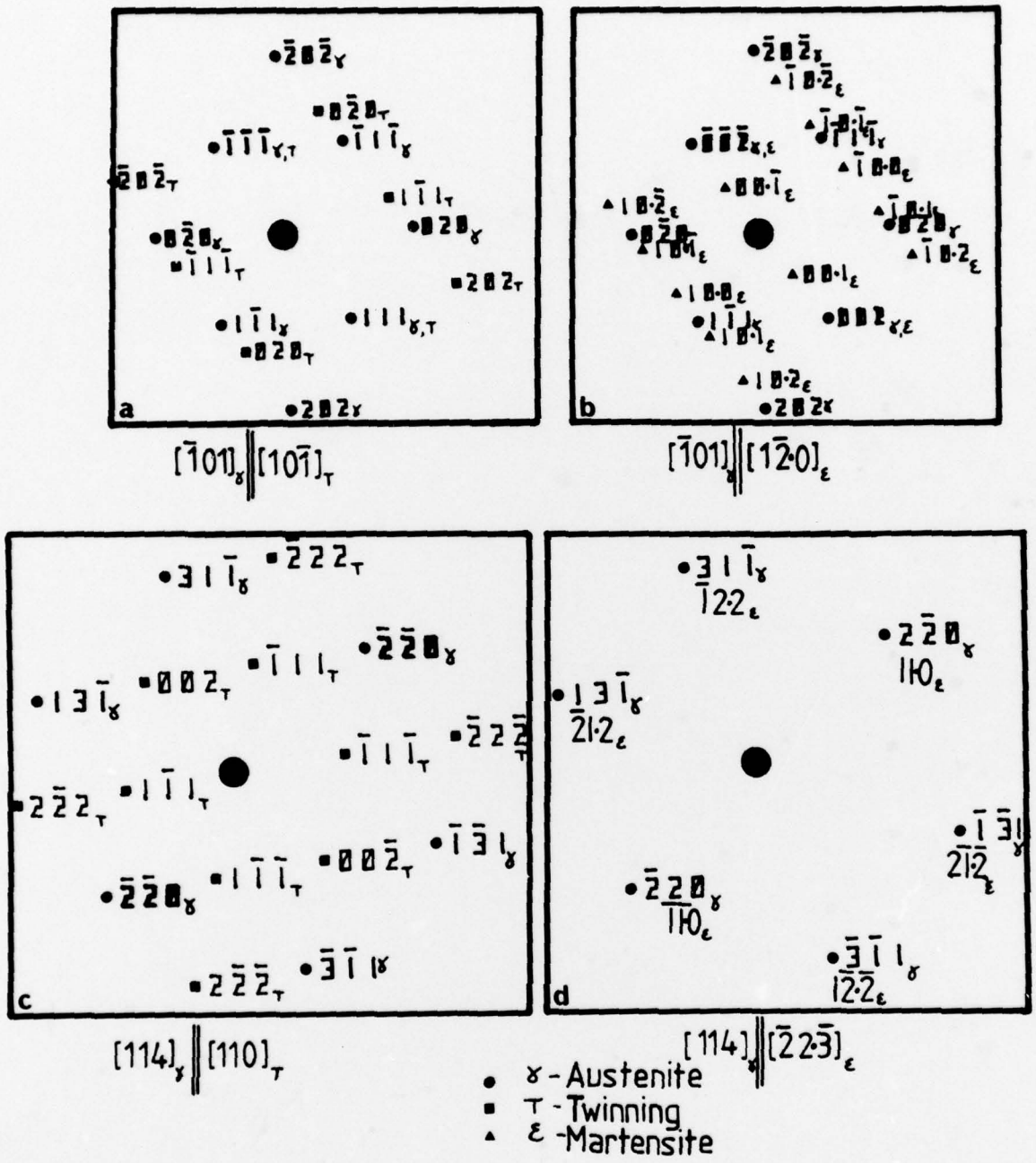

AERE - R 9361 Fig. 8

Superimposed computer-simulated electron diffraction patterns for the fcc γ/twinning and fcc γ/hcp ε relationships in the $[\bar{1}01]_\gamma$ ((a) and (b)) and $[114]_\gamma$ ((c) and (d)) matrix orientations